

Low-lying quasiparticle states and hidden collective charge instabilities in parent cobaltate superconductors (Na_xCoO_2)

D. Qian,¹ D. Hsieh,¹ L. Wang,¹ A. Fedorov,² D. Wu,³ J. L. Luo,³ N. L. Wang,³ L. Viciu,⁴ R. J. Cava,⁴ and M. Z. Hasan^{1,5}

¹Department of Physics, Joseph Henry Laboratories of Physics, Princeton University, Princeton, NJ 08544

²Advanced Light Source, Lawrence Berkeley Laboratory, Berkeley, CA 94305

³Institute of Physics, Chinese Academy of Sciences, Beijing 100080, China

⁴Department of Chemistry, Princeton University, Princeton, NJ 08544

⁵Princeton Center for Complex Materials, Princeton University, Princeton, NJ 08544

(Dated: March 23, 2024)

We report a state-of-the-art photoemission (ARPES) study of high quality single crystals of the Na_xCoO_2 series focusing on the fine details of the low-energy states. The Fermi velocity is found to be small ($< 0.5 \text{ eV \AA}$) and only weakly anisotropic over the Fermi surface at all dopings setting the size of the pair wavefunction to be on the order of 10-20 nanometers. In the low doping regime the exchange inter-layer splitting vanishes and two dimensional collective instabilities such as 120-type fluctuations become kinematically allowed. Our results suggest that the unusually small Fermi velocity and the unique symmetry of kinematic instabilities distinguish cobaltates from other unconventional oxide superconductors such as the cuprates or the ruthenates.

PACS numbers: 71.20.b, 73.20.At, 74.70.b, 74.90.+n

Research on strongly correlated electron systems has led to the discovery of unconventional states of matter such as those realized in the high T_c superconductors, quantum Hall systems and low-dimensional quantum magnets. Triangular cobaltates Na_xCoO_2 are a novel class of correlated electron systems with a rich phase diagram. Superconductivity (near $x = 1/3$) and correlated insulator behavior ($x = 1/2$) are observed in the low doping regime and enhanced thermoelectric power (near $x = 2/3$) and an unusual spin-density-wave state (beyond $x = 3/4$) are seen in the high doping regime [1]–[3]. None of the existing theories of cobaltates can account for the changes of electronic groundstates with doping, and no systematic study of its low-energy dynamics (e.g., Fermi velocity, inter-layer coupling, particle-hole instabilities etc.) exists so far.

An early ARPES study [4] carried out on the host compound found only one Fermi surface (FS), however the fine details of the quasiparticles were not resolved. A subsequent study by Yang et al. [5], reported a surface state with a large FS and broad bulk-representative quasiparticles due to the surface annealing process but only one bulk FS was observed reconciling the finding in Ref. [4]. In this Letter, we report the fine details of the low-energy quasiparticle states which allow us to determine the dimensionality and the kinematic instabilities associated with the electronic structure as a function of doping as well as the fundamental parameters to compare the electron dynamics with other unconventional superconductors. Such a study is made possible due to the lack of surface reconstruction (hence no surface state complications in the interpretation of the data) in our high quality crystals. The strong interlayer coupling we resolve in the high doping regime provides evidence for a natural mechanism for the unusual magnetic order observed,

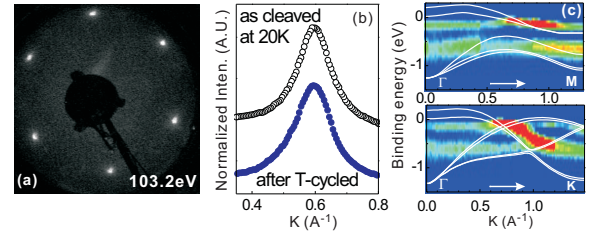


FIG. 1: (a) Low energy electron diffraction image of the cleaved (001) surface exhibits hexagonal symmetry of the cobalt layers. No Ruthenate-like surface reconstruction is observed. (b) Temperature cycling (20K \leftrightarrow 100K) was found to have no effect on the momentum distribution (MDCs) of the quasiparticles. Only one peak is observed at $x = 0.57$ and lower dopings. (c) The valence band overlaid with band calculations [6] shows narrowing due to electron correlations.

even though the system is far away from the conventional half-filled Mott limit ($x = 0$). In contrast, the details of the low-energy behavior in the low doping regime ($x = 1/3$) reveal a hidden two dimensional particle-hole instability predicted in recent many-body theories. Moreover, the results allow us to reliably compare the low-energy parameters obtained on cobaltates with other materials classes and provide fundamental ingredients for developing a microscopic theory of these materials.

Spectroscopic measurements were performed with 30 eV to 90 eV photons with better than 10 to 25 meV energy resolution, and angular resolution better than 0.8% of the Brillouin zone at ALS Beam lines 12.0.1 and 10.0.1, using Scienta analyzers with chamber pressures below 4×10^{-11} torr. High quality single crystals over a wide doping range $x = 0.3, 0.33, 0.52, 0.57 (\text{Na/K}), 0.7, 0.75$ and 0.79 were used for this study. Cleaving the samples

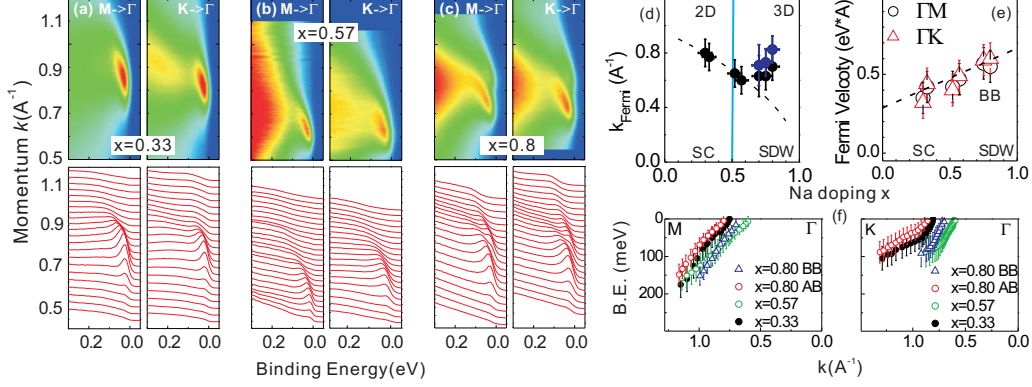


FIG. 2: Evolution of low-lying quasiparticle states: Single-particle momentum-resolved photoemission spectra for $x = 0.33$ (a), $x = 0.57$ (b) and $x = 0.80$ (c) along the Γ -M and Γ -K cuts. Low doped samples (a,b) exhibit only one Fermi crossing while high doped samples (c) show two Fermi crossings. Doping evolution of Fermi surface size (k_F) is shown in (d) and Fermi velocity in (e). Fermi velocity increases with increasing doping. Bonding (BB) and antibonding (AB) bands are identified at high doping. Note that the average $(BB + AB)$ Fermi velocity decreases in approaching $x = 1$. The dotted line in (d) is calculated based on the 2-D Luttinger theorem [4]. (f) Band dispersion plots along the Γ -M and Γ -K cuts.

in situ at 20 K (or 100 K) resulted in shiny flat surfaces, characterized by diffraction to be clean and well ordered with the same symmetry as the bulk (Fig-1). No surface state was observed. All presented data were taken at 20 K, although in a few cases samples were studied at 100 K for cross-checking.

Fig-2 shows the doping dependence of single electron momentum-resolved photoemission spectra as a function of energy and momentum. For low doping ($x < 2/3$), one quasiparticle feature is seen to disperse from high binding energies at high momentum values near the corner (K) or the face (M) of the reciprocal space to the Fermi level. High resolution study of the quasiparticle feature shows that it is well separated from the hump structure observed at 200–300 meV binding energies at all doping. The quasiparticle lifetime drops very fast making its intensity vanish beyond 70 to 100 meV binding energies depending on the doping. The low energy (0–50 meV) Fermi velocities extracted from the data are shown in Fig-2 (e). The Fermi velocity is found to be weakly anisotropic, (e.g., similar in magnitude along Γ -M, and Γ -K directions) at all doping levels, and increases with doping away from the Mott limit ($x = 0$). The Fermi velocity, averaged over the FS, is about 0.37 eV Å for $x = 0.3$. Given the size of the FS, we estimate the carrier mass, $m^* = \hbar k_F / v_F$ is 15 to 30 m_e . This is rather large compared to most known transition metal oxide superconductors. However, a similarly large carrier mass ($m^* \sim 70 m_e$) has recently been reported by SR measurements [7]. Fig-2 (d) plots the average size of the Fermi surface (k_F) as a function of doping. Doping evolution is found to follow the 2-D Luttinger theorem (FS area / $(1-x)$) up to x near 2/3. The Fermi surface (k_F) gets broadened and splits into two clearly separate ones beyond $x = 0.7$.

Fig-3 (a) shows the momentum-distribution ($n(k)$ -plot) for $x = 0.33$ as a representative of the low-doping regime. The inner edge of this density plot is the Fermi surface. The electron distribution in the extended zone scheme is shown in Fig-3 (b). In Fig-4 we show the quasiparticle behavior in a typical high doping ($x > 2/3$) sample. Two quasiparticles are observed to cross the Fermi level with the k -splitting. A systematic study shows coupled oscillatory behavior of quasiparticle peak intensities with increasing incident photon energy. This is commonly observed for states with nearly orthogonal symmetries [8]. The unit cell of Na_xCoO_2 has two Co-layers – therefore the Co-derived bands with orthogonal symmetries are expected to be split, leading to two Fermi crossings similar to what is observed in multi-layer materials [8, 9]. Inter-layer splitting in cobaltates has been predicted by LDA band theory [6]. It is known from neutron and x-ray diffraction studies that with increasing Na content the separation between the two cobalt layers decreases substantially [10, 11]. Filling of the Na layer by high Na density (high doping) leads to stronger bonding between the Co layers resulting in decreased interplanar (c -axis) distance. Therefore, our observation of inter-layer splitting at high doping and its absence at low doping suggest a two to three dimensional crossover of the low-lying electronic structure with increasing sodium concentration. The large interlayer splitting observed only at high x suggests that c -axis exchange is large, since inter-layer hopping and magnetic exchange (exchange inter-layer) are directly related ($J_z \propto t_z^2$). The crucial role of the Na-layer (atomic rearrangements) at high doping in determining the magnetic state of the sample is thus consistent with recent NMR findings [13].

The Fermi surface area at high doping does not ex-

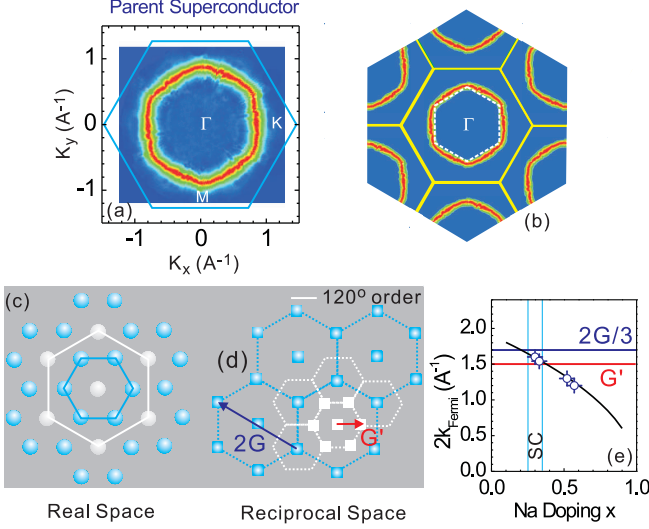


FIG. 3: Fermi Surface and Collective Instabilities: (a) Momentum distribution of electrons in the $x=0.33$ sample measured in a simultaneous azimuthal scan mode with an energy window of 10 meV. (b) Electron distribution shown in an extended zone scheme. (c,d) Real-space arrangement of cobalt atoms and 120° type order and their corresponding reciprocal lattices. (e) Average electron-hole excitation wave-vector ($2k_F$) as a function of Na doping x . In the low doping regime, the measured data points (open circles) fall on the 2-D Luttinger theorem (solid) line. Horizontal solid lines represent two commensurate instabilities. The 120° order line (G^0 , red) intersects the ($2k_F$)-line near $x=0.34$ and the $2G/3$ lattice vector line intersects near $x=0.25$ enclosing the superconducting phase boundaries [22].

actly match the 2-D Luttinger count (deviation of data from the dotted line in Fig-2 (d)). The fact that the Fermi velocity and other band behavior exhibit systematic changes with doping suggests that the deviation can not be due to doping inhomogeneity. We attribute this deviation in FS area to two factors which were overlooked in earlier studies. The SDW order leads to a canonical doubling of the primitive unit cell, and since the order is fully 3-D, a projected or quasi-2D map of the FS does not necessarily capture the full volume. Thus the 2-D Luttinger count is not applicable to the FS of highly doped cobaltates, where a 3-D SDW is observed. This fact and the unresolved bilayer splitting provide clues to the puzzle of the reported FS being larger in previous studies [4, 5]. To perform a proper Luttinger count one would need to count the full 3D Fermi surface volume and consider the effect of the full SDW order on the electronic structure.

Based on the vanishing of interlayer coupling in going from high to low doping, we conclude that the electronic structure is largely two dimensional near the supercon-

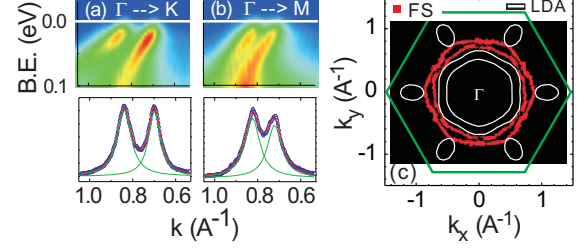


FIG. 4: (a,b) A two-band (double) crossing behavior is observed for $x > 2/3$. Systematics of data are shown for $x=3/4$ where samples exhibit 3-D SDW order. The data can be modeled with two Lorentzians. (c) The Fermi surface topology is compared with inter-layer splitting in LDA calculation [6]. The observed FS "consumes" the area of the corner pockets.

ducting Na concentration. We now discuss the possibility of electron-hole excitation induced instabilities with 2-D commensurate wave vectors. We note that the 2-D FS near $x=1/3$ exhibits nearly straight sections perpendicular to the high symmetry directions. At low doping, this distance $2k_F$ is very close to $2G/3$, where G is the fundamental reciprocal lattice vector (Fig-3). However, this vector can not nest the pieces of the FS we observe. Another instability is that of the 120° type which can arise from weak spatial modulations of charge, spin or orbital densities. Our data shows that the electronic system in the vicinity of $x=1/3$ is susceptible to such kinematic instabilities. This is due to the fact that the BZ of such order or fluctuations coincides with the topology of our measured FS. The geometrical construct for 120° order is shown in real and reciprocal space in Fig-3 (c) and 3 (d). The Brillouin zone constructed out of the white hexagons in Fig-3 (d) is superimposed on the measured Fermi surface (white hexagon) presented in Fig-3 (b). The coincidence, including the k -space anisotropies, can be noted in Fig-3 (b). For this type of instability there is no specific nesting vector and the instability is collective in nature involving all parts of the FS. In order to determine whether or not this instability is unique to $x=0.3$, we have carried out the doping dependence of FS size in the vicinity of $x=0.3$. The uniqueness of this instability (G^0) can be seen in Fig-3 (e) – the $G^0 = 2k_F$ line intersects the Luttinger line uniquely near $x=0.34$, which is the doping for superconductivity [22].

The doping evolution of electron behavior and low-energy correlation effects have been theoretically studied in an extended Hubbard model on a triangular lattice [14]. These studies predict strong renormalization of bandwidth (i.e., small Fermi velocity) over the phase diagram. Moreover, a strictly two dimensional 120° -type collective instability or order, such as $\sqrt{3} \times \sqrt{3}$, near $x=1/3$ and $2/3$ is predicted. Our results show that only near $x=1/3$ is such a two dimensional instability (with tri-

TABLE I: Comparison of cobaltates with Bardeen-Cooper-Schrieffer (BCS) and non-BCS cuprate superconductors

Class	T_c (K)	Fermi velocity (eV/Å)	Retardation [17] $\frac{E_{fermi}(W)}{h\hbar\omega_{ph}(opt)}$ (by Phonons)	Phase Ordering [17,18,21] T (K) $n_{2d}(S_F) = m$	Mass $\frac{m}{m_e}$ $\frac{\hbar k_{fermi}}{m_e}$	Size of the Pair Wave fn (Å) $0.2 \frac{\hbar v_{fermi}}{k_B T_c}$	Ref.
Cobaltates (NaCoO ₂)	5	0.37-0.1	< 4	< 20	> 15	200	Present work
p-Cuprates (LaSCO)	38	1.8	8	54	2 (nodal)	100	[16,17]
n-Cuprates (NCCO)	21	2.0	9	130	2.4 (nodal)	210	[16,17]
MgB ₂	39	2-7	10 ²	10 ³	x	x	[19]
Lead (Pb)	7.2	10.4	10 ³	10 ⁵	1.8	10 ⁴	[17,20]

angular symmetry) allowed with the measured topology of the Fermi surface (Fig-3). Near $x=2/3$ on the other hand, electronic structure is three dimensional. Theory suggests that if this order is long-range, the quasiparticle spectrum would be gapped at all momenta (k) and the Fermi velocity would exhibit strong renormalization at nearby dopings. In our study, no gap opening is observed in the quasiparticle dispersion (Fig-2(a)) at any momentum at this doping down to the base temperature of the experiment. However, the Fermi velocity is seen to be suppressed over a range of doping (Fig-2(e)). Therefore, our results suggest a strongly fluctuating character of this collective instability [22].

The strong correlation models have further been considered in connection with superconductivity [14, 15]. These studies suggest that a kinematic or hidden FS instability with strong fluctuations can lead to unconventional superconductivity with an f -wave order parameter, even within a Fermi-liquid quasiparticle-like picture. The quasiparticle parameters related to the cobalt derived states with triangular symmetry are therefore of interest for theory. Based on our data, we estimate the parameters in cobaltates presented in Table-I. For comparison we also quote similar parameters obtained on conventional materials as well as the unusual materials classes. For use in Table-I, the Fermi energy of cobaltates is estimated to be on the order of the occupied bandwidth (following the approximation in ref.[17]) which is taken from our data in Fig-2(f). At the order-of-magnitude level, our results show that the cobaltate exhibits a lack of a retardation effect due to its small Fermi energy, possesses a small phase ordering (kinetic energy) scale due to its large effective mass, and exhibits a relatively short coherence length (Cooper pair wavefunction) due to its small Fermi velocity (consequence of uncertainty relation). All these characteristics can be traced to the strong renormalization of the Fermi velocity which, in cobaltates, is about a factor of five smaller than it is in the high T_c cuprates. Given such character for the low-lying states and the k -space kinematics we observe, it is unlikely that a conventional mechanism is at play.

In conclusion, the details of the low-energy states in

Na_xCoO₂ are resolved due to high crystalline quality of materials. A splitting of the single-particle band signalling inter-layer coupling is observed in the high doping regime which accounts for the observed three dimensional magnetism. In the low doping regime, in contrast, the splitting disappears leading to the two dimensional character of triangularly correlated electron motion. Our results suggest that the strongly renormalized Fermi velocity and the unique two dimensional symmetry of kinematic instabilities distinguish cobaltates from most other oxide superconductors and clearly so from BCS superconductors. The quantitative details of the low-lying states in our studies (Table-I) provide important guides to develop a comprehensive theory of cobaltates.

We gratefully acknowledge P.W. Anderson, D.A. Huse, S.A. Kivelson, P.A. Lee, N.P. Ong, S. Shastri and S. Sondhi for discussions. This work is partially supported through the NSF (DMR-0213706), DOE (DE-FG02-05ER46200 and DE-FG02-98-ER45706) and NSFC (10574158).

-
- [1] K. Takada et al, Nature 422, 53 (2003).
 - [2] I. Terasaki et al, Phys. Rev. B 56, R12685 (1997).
 - [3] N.P. Ong and R.J. Cava, Science, 305, 52 (2004).
 - [4] M.Z. Hasan et al, Phys. Rev. Lett. 92, 246402 (2004); cond-mat/0501530 (2005).
 - [5] H.B. Yang et al, Phys. Rev. Lett. 95, 146401 (2005).
 - [6] D.J. Singh, Phys. Rev. B 61, 13397 (2000).
 - [7] A. Kaniyel et al, Phys. Rev. Lett. 92, 257007 (2004).
 - [8] Y.-D. Chuang et al, Phys. Rev. Lett. 87, 117002 (2001).
 - [9] D.L. Feng et al, Phys. Rev. Lett. 86, 5550 (2001).
 - [10] Q. Huang et al, Phys. Rev. B 70, 184110 (2004).
 - [11] M. Foo et al, Phys. Rev. Lett. 92, 247001 (2004).
 - [12] S.P. Bayrakci et al, Phys. Rev. Lett. 94, 157205 (2005).
 - [13] C. de Vaulx et al, Phys. Rev. Lett. 95, 186405 (2005).
 - [14] O. Motunich, P.A. Lee, Phys. Rev. B 70, 024514 (2004).
 - [15] Y. Tanaka et al, cond-mat/0311266 (2003).
 - [16] A. Damascelli et al, Rev. Mod. Phys. 75, 473 (2003); A. Kaminski et al, Phys. Rev. B 71, 014517 (2005).
 - [17] E.W. Carlson et al, "The Physics of Conventional and Unconventional Superconductors," ed. K.H. Bennemann and J.B. Ketterson (Springer-Verlag, 2002).

- [18] V. Emery, S.A. Kivelson, *Nature*, 374, 434 (1995).
- [19] H. Uchiyama, et al., *Phys. Rev. Lett.* 88, 157002 (2002).
- [20] K. Hom et al., *Phys. Rev. B* 30, 1711 (1984).
- [21] Since the superfluid density is not known we have used the Fermi sea to calculate the phase ordering scale at the order of magnitude level.
- [22] We note a natural enlargement of the central FS at $x=1/3$ in our data (Fig-3) with respect to LDA predictions given

the absence of corner FS pockets (Ref.[4,5]) and the constraint of the Luttinger theorem. Therefore, 120 type kinematic instabilities are seen to be only allowed in the absence of the corner pockets. Remarkably, our results suggest that both the suppression of corner pockets and the enhanced susceptibility to 120 type order are natural consequences of long-range Coulomb interactions.